Low-Dimensional Models For Feedback Flow Control. Part I: Empirical Galerkin models[*]

Bernd R. Noack[†]

Technical University of Berlin HF1, Straße des 17. Juni, 10623 Berlin, Germany

Gilead Tadmor[‡]

Northeastern University, 440 Dana Research Building, Boston, MA 02115, U.S.A.

Marek Morzyński[§]

Poznan University of Technology, Piotrowo 3, 60-965 Poznan, Poland

A flow model which is accessible to control design must combine low dimension, robustness and a simple structure with an ample dynamic range to cover controlled transients. Key enablers are reviewed in the context of empirical Galerkin models and are exemplified for incompressible shear flows. These enablers include 'subgrid' turbulence and pressure representations, hybrid models that combine multiple operating points, and actuation models. The range of model validity is identified in terms of invariant manifolds which can be exploited by observer design and has to be respected by controller design.

Nomenclature

$\mathbf{x}$	Location
$\hat{\mathbf{e}}_x, \hat{\mathbf{e}}_y, \hat{\mathbf{e}}_z$	unit vectors in x-, y-, and z-direction
x, y, z	Cartesian coordinate system
Ω	Domain
y_{cyl}	Transverse position of the cylinder
t	Time
$\mathbf{u}, \mathbf{v}$	Velocity fields
$\mathbf{u}_0$	Base flow (mostly: averaged velocity field)
$\mathbf{u}'$	Fluctuation of the velocity field
$\mathbf{u}'_{\mathrm{inhom}}$	Wall-imposed fluctuation
$\mathbf{u}'_{\mathrm{hom}}$	Free fluctuation (flow response)
p	Pressure field
$\mathbf{g}_\alpha$	α-th volume force
Γ_α	Amplitude of α-th volume force
N_Γ	Number of volume forces
Re	Reynolds number
ν	Reciprocal of Reynolds number
$\mathbf{u}_i$	i-th actuation mode for $i < 0$; i-th expansion mode for $i > 0$
$\mathbf{u}^{[N]}$	Galerkin approximation with N modes

a_i	Fourier coefficient of the i-th mode
N, N_{EM}	Number of expansion modes
N_{KL}	Number of Karhunen-Loeve modes
N_A	Number of actuation modes
$l_{ij}, q_{ijk}, g_{i\alpha}$	Galerkin system coefficients
l_{ij}^+, q_{ijk}^+	Galerkin system coefficients for additional physics processes
	(turbulence and pressure representation)
$\nu_{T,i}$	Modal eddy viscosity associated with the i-th mode
δ_{ij}	Kronecker symbol

I. Introduction

A framework is presented for the construction of low-dimensional Galerkin models targeting feedback flow control applications. The feedback component is necessary for the low-amplitude suppression of instabilities, like the reduction of vortex shedding.[1–3] Energy-effective amplification of coherent structures may also benefit from a feedback component. These benefits include the stretching of the dynamic range of operating conditions and the consideration of unmodelled dynamics like disturbances and off-design conditions.[4,5]

Feedback flow control applications are designed to manipulate coherent structures for the control goal. This manipulation has many degrees of freedom in actuation, sensing, and control design. Examples are the choice of the kind of actuators, their placement, their operating frequency and amplitude range, in addition to similar decisions for the sensor. However, the exploration of good actuation, sensing, and control solutions with high-dimensional computational fluid dynamics models is prohibitively expensive. In addition, practical feedback design requires a low dimension of the model excluding a CFD flow model. Therefore, low-dimensional models of the coherent structures are sought as practicable enablers.

The empirical Galerkin method based on a Karhunen-Loève decomposition of flow data offers an efficient path to control-oriented models.[6] The promise of the method is that the resulting model predicts the actuation effect on a neighborhood of flow states, i.e. describes more than the reference simulation. However, the standard empirical Galerkin model (as described in Ref. 7) is known to be over-optimized for the reference data.[8] Significant advances to overcome this shortcoming have been made in recent years. These advances allow to extend the dynamic range of the model[9–13] and to incorporate actuation.[14–16] A low-dimensional flow representation allows also to identify good sensor locations.[17,18]

The current manuscript describes key enablers to enhance the applicability of empirical Galerkin models for model-based feedback flow control. The manuscript is organized as follows: In §II, the 'standard' Galerkin method is reviewed. A toolbox with generalizations is described in §III. The toolbox include a pressure-term representation, a 'subgrid' turbulence representation, non-equilibrium modes, and actuation models. Their necessity is illustrated for the laminar shear-layer (§IV), the turbulent mixing layer (§V), the transient cylinder wake (§VI), and the actuated cylinder wake (§VII). The main findings are summarized in §VIII. The discussed Galerkin modelling toolbox is employed in a feedback flow control study which is described in a companion paper (Part II) at this conference.[19] That paper proposes also methods for controller design and dynamic estimation.

II. Galerkin method

In this section, the 'standard' empirical Galerkin method is reviewed.

A flow model is expected to approximate the solution of an initial boundary value problem for the velocity $\mathbf{u}$ and the pressure field p subject to suitable boundary and initial conditions. The non-dimensionalized evolution equation consists of the continuity equation,

$$\nabla \cdot \mathbf{u} = 0, \tag{1}$$

and the Navier-Stokes equation,

$$\partial_t \mathbf{u} + \nabla \cdot (\mathbf{u}\,\mathbf{u}) = -\nabla p + \nu \triangle \mathbf{u}, \tag{2}$$

where the reciprocal of the Reynolds number is denoted by $\nu := 1/Re$.

The velocity field in the physical domain Ω is approximated by a finite expansion in terms of N space-

dependent *expansion modes* $\mathbf{u}_i$ and the corresponding time-dependent *Fourier coefficients* a_i,

$$\mathbf{u}(\mathbf{x}, t) \approx \mathbf{u}^{[N]}(\mathbf{x}, t) := \sum_{i=0}^{N} a_i(t)\, \mathbf{u}_i(\mathbf{x}). \tag{3}$$

For later reference, a *basic mode* $\mathbf{u}_0$ with amplitude $a_0 \equiv 1$ is included.

This ansatz includes the *computational* Galerkin method[20] which is based on expansion modes with a local compact support on grid cells, e.g. FEM 'hats'. Their advantage is to describe a large class of transient solutions from different initial conditions. The price is a high dimension.

We trade generality and accurateness for low dimension and robustness and follow the *traditional* Galerkin method.[20] This method is based on a Hilbert space for the fluctuation $\mathbf{u}' := \mathbf{u} - \mathbf{u}_0$. A typical choice of the Hilbert space is the set of square-integrable solenoidal vector fields $\in \mathcal{L}^2(\Omega)$ with the corresponding inner product between two vector fields $\mathbf{u}$, $\mathbf{v}$,

$$(\mathbf{u}, \mathbf{v})_\Omega := \int_\Omega dV\, \mathbf{u} \cdot \mathbf{v}. \tag{4}$$

Orthonormality, i.e. $(\mathbf{u}_i, \mathbf{u}_j)_\Omega = \delta_{ij}$, and smoothness imply that the modes are *global*, i.e. are non-vanishing almost in the whole domain Ω. Moreover, the definition of these modes are independent of a grid.

The *empirical* Galerkin method[6,7] based on the Karhunen-Loève decomposition leads — by construction — to the least-dimensional representation of a single operating condition determined by the reference simulation. We do not follow *mathematical*[21] or *physical*[22] Galerkin approaches, since they are too high dimensional and less applicable for complex geometries.

In the traditional Galerkin method, the evolution equation of the Fourier coefficients is derived from the Galerkin approximation (3) by a Galerkin projection of the Navier-Stokes equation (2) onto the expansion modes $\mathbf{u}_i$.[7] The resulting *Galerkin system* has the form

$$\frac{d}{dt} a_i = \nu \sum_{i=0}^{N} l_{ij} a_j + \sum_{i=0}^{N} \sum_{j=0}^{N} q_{ijk} a_j a_k, \tag{5}$$

where $l_{ij} := (\mathbf{u_i}, \triangle \mathbf{u}_j)_\Omega$ and $q_{ijk} := (\mathbf{u_i}, \nabla \cdot [\mathbf{u}_j\, \mathbf{u}_k])_\Omega$. Typically, the pressure term is neglected — often for justifiable reasons.

The empirical Galerkin model (3,5) may accurately reproduce the reference simulation in a low-dimensional manner. However, the model tends to be over-optimized for that reference condition. In particular, the performance tends to rapidly deteriorate with changes of Reynolds number[8] or even in the neighborhood of the attractor.[11,23] Current modelling efforts by this team are directed towards exploiting the low-dimensionality of the empirical approach and enhancing the range of validity by incorporating select information contained in physical or mathematical models.

III.   Toolbox for control-oriented models

Control applications suggest 6 minimum requirements for such a control-oriented model (Fig. 1). These properties include a dynamics representation for

(a) the natural flow (I) as initial condition,

(b) the actuated flow (II) not far from the desired controlled flow,

(c) the natural transient from (II) to (I), i.e. the transient when actuation is turned off,

(d) the actuated transient from (I) to (II),

(e) the suitability of the model for control design, and

(f) the possibility of observer design from one or more sensor signals.

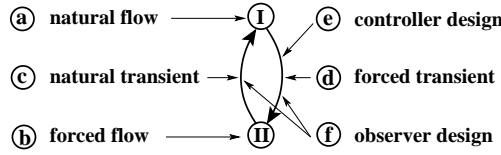American Institute of Aeronautics and Astronautics Paper 2004-2408

Figure 1. Minimum requirements for a Galerkin model which shall be suitable for control design.

From requirements (a–d), the model may be expected to describe actuation effects in the neighborhood of the natural (I) and the actuated flow (II). In that range of validity, the model may replace more expensive Navier-Stokes simulations for control design purposes and for exploratory actuation studies.

The Galerkin ansatz (3) with $N_{KL} = N$ Karhunen-Loève modes may resolve the coherent-structure dynamics of the reference operating condition. However, the Karhunen-Loève decomposition at one operating condition, e.g. one Reynolds number, cannot be expected to be accurate at another condition, e.g. another Reynolds number.[8] Both, the mean flow and the Karhunen-Loève modes change with flow parameters and actuation, as illustrated in Fig. 2a.

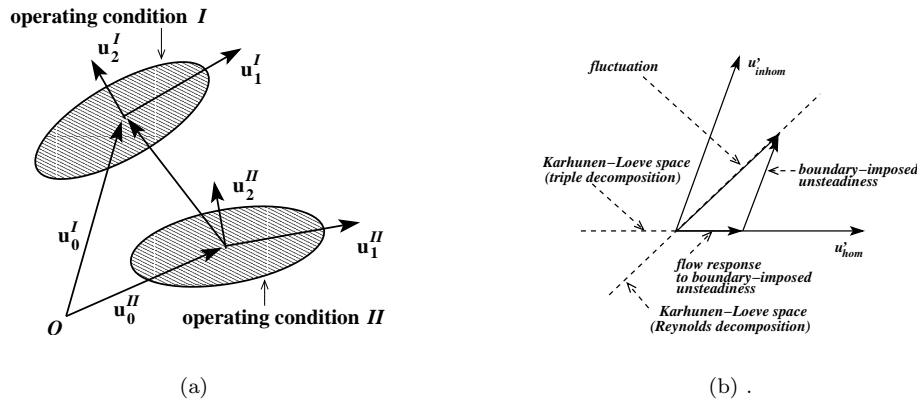(a)   (b) .

Figure 2. Principal sketch of the decompositions leading to the modes in Fig. 3. Fig. (a) shows Karhunen-Loève decompositions at two different operating conditions (I) and (II). Fig. (b) illustrates the Karhunen-Loève decomposition based on the boundary-imposed unsteadiness $\mathbf{u}'_{\text{inhom}}$ satisfying the inhomogeneous boundary condition and the flow response $\mathbf{u}'_{\text{hom}}$ obeying the homogenized boundary condition.

One straight-forward approach to describe two or more operating conditions in a single ansatz consists by adding *non-equilibrium modes* $\mathbf{u}_i$, $i = N_{KL} + 1, \ldots, N_{EM}$ in the expansion.[10, 11] Orthonormality is enforced in the enlarged set of N_{EM} expansion modes. Note that the order of the included operating condition affects the individual expansion modes but does neither change the Galerkin space spanned by the generalized ansatz nor the dynamics of the Galerkin system. Snapshot ensembles comprising several operating conditions[9] or the transients under chirp forcing[13] serve the same purpose.

The effect of acoustic actuators, moving walls, or oscillating free-stream is hardwired to the flow response — even in the generalized Galerkin approximation. To design this form of actuation as a free control input, the fluctuation is decomposed in a *boundary-imposed unsteadiness* $\mathbf{u}'_{\text{inhom}}$ satisfying an inhomogeneous boundary condition and a *flow response* $\mathbf{u}'_{\text{hom}}$ (see Fig. 2b). The imposed unsteadiness is modelled by N_A *actuation modes* $\mathbf{u}_i$, $i = -N_A, \ldots, -1$ and their amplitudes are a free control input.[14–16] Note that this decomposition is far from being unique and that the choice affects the Karhunen-Loève space and hence all other expansion modes.

Summarizing, the generalized Galerkin approximation consistent with requirements (a-d) is expressed by

$$\mathbf{u} = \sum_{i=0}^{N_{KL}} a_i \, \mathbf{u}_i + \sum_{i=N_{KL}+1}^{N_{EM}} a_i \, \mathbf{u}_i + \sum_{i=-N_A}^{-1} a_i \, \mathbf{u}_i. \tag{6}$$

The role of the modes is summarized in Fig. 3a. The resulting generalized Galerkin system is obtained from

American Institute of Aeronautics and Astronautics Paper 2004-2408

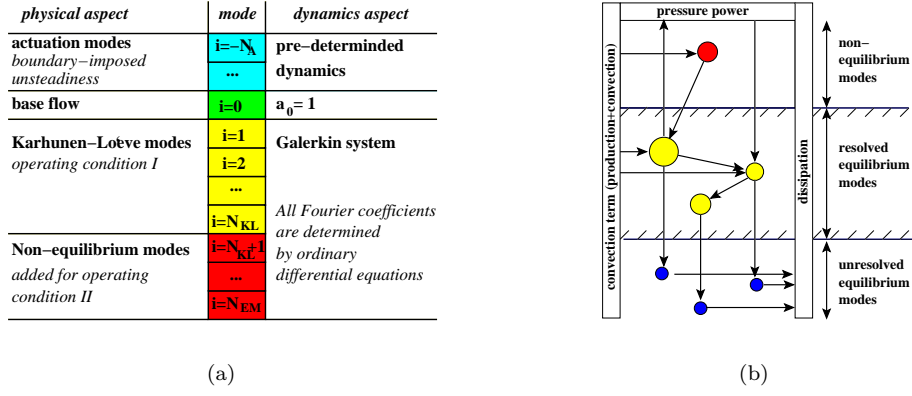| physical aspect	mode	dynamics aspect
actuation modes *boundary–imposed unsteadiness*	$i=-N_A$ ...	**pre–determined dynamics**
base flow	$i=0$	$a_0 = 1$
Karhunen–Loève modes *operating condition I*	$i=1$ $i=2$ ... $i=N_{KL}$	**Galerkin system** *All Fourier coefficients are determined by ordinary differential equations*
Non–equilibrium modes *added for operating condition II*	$i=N_{KL}+1$ ... $i=N_{EM}$	

(a)

(b)

Figure 3. Principal sketch of the expansion modes including the physical, dynamical and energetic role. In Fig. (a) the modes used in this study are enumerated and explained. In Fig. (b) the energetic role of the expansion modes is elucidated. Each mode is visualized by a circle and the corresponding energy flows by arrows. Arrows connecting the mode with the convection term, with the dissipation, and with pressure power box represent the sum of modal production and convection, the modal dissipation, and the modal pressure power, respectively. Arrows between the modes contribute to the transfer term. The direction of the arrow is aligned with the direction of the energy flow. The non-equilibrium modes vanish in the long-term limit without forcing.

a straight-forward Galerkin projection,

$$\frac{d}{dt}a_i = \nu \sum_{i=-N_A}^{N} (l_{ij} + l_{ij}^+)\, a_j + \sum_{i=-N_A}^{N} \sum_{j=-N_A}^{N} (q_{ijk} + q_{ijk}^+)\, a_j a_k + \sum_{\alpha=-N_A}^{-1} g_{i\alpha}\, \frac{da_i}{dt} + \sum_{\alpha=1}^{N_\Gamma} g_{i\alpha}\, \Gamma_\alpha. \qquad (7)$$

The α-th actuation mode gives rise to an acceleration term $g_{i\alpha}\, da_\alpha/dt$ in the i-th evolution equation, where $g_{i\alpha} := (\mathbf{u_i}, \mathbf{u}_\alpha)_\Omega$, $\alpha = -N_A, \ldots, -1$.

Eqn. (7) incorporates also a Galerkin representation of the N_Γ volume forces $\Gamma_\alpha\, \mathbf{g}_\alpha$. That representation is the term $\Gamma_\alpha g_{i\alpha}$, where $g_{i\alpha} := (\mathbf{u_i}, \mathbf{g}_\alpha)_\Omega$, $\alpha = 1, \ldots, N_\Gamma$.

The Galerkin system coefficients l_{ij}, q_{ijk} are derived from the viscous and convective Navier-Stokes term in complete analogy to Eqn. (5). The additional coefficients l_{ij}^+, q_{ijk}^+ allow to incorporate new physics processes. One example is the 'subgrid' turbulence representation for the effect of dynamically unresolved fine-scale Karhunen-Loève modes $i > N_{KL}$. As indicated in Fig. 3b, these modes tend to act as energy sinks on the resolved modes via the transfer term. This dissipative effect can be linearly modelled by a modal eddy viscosity,[24]

$$l_{ij}^+ := \nu_{T,i}\, l_{ij}.$$

The eddy viscosity $\nu_{T,i}$ is uniquely determined by a modal energy flow balance.[25]

Another example for physical process is the pressure term[12, 26, 27] which is described by additional quadratic Galerkin system coefficients q_{ijk}^+. It should be noted that a model calibration for one operating condition may or may not be applicable to another operating condition.

Table 1 summarizes the discussed generalizations of the empirical Galerkin model as a toolbox.

IV.   Laminar mixing layer

The necessity of the pressure model in the Galerkin ansatz is exemplified for the Kelvin-Helmholtz vortices in the 2D shear layer (see Fig. 4a). The Reynolds number is 150 based on the maximal velocity and the initial vorticity thickness. The streamwise size of the computational domain covers 2 wavelengths. Details of the corresponding simulation and model are discussed in Refs. 26, 27.

A four-dimensional energy-resolving empirical Galerkin model is constructed for this periodic flow. The first 2 Karhunen-Loève modes describe 99.5% of the fluctuation energy. Higher Karhunen-Loève modes resolve higher harmonics and have a small energy content since the fluctuation amplitude at the inflow boundary is 1% and non-linearity is insignificant in the considered regime.

Table 1. Generalizations of the 'standard' Galerkin model

| aspect	generalization of the Galerkin approximation — kinematics —	generalization of the Galerkin system — dynamics —
flow	non-equilibrium modes, e.g. • shift mode • stability eigenmodes [task b–d of Fig. 1]	pressure-term representation, e.g. • analytical model • empirical model 'subgrid' turbulence model, e.g. • single eddy viscosity • modal eddy viscosities [task a of Fig. 1]
actuation	actuation models, e.g. • actuation mode for boundary-imposed unsteadiness [task b,d of Fig. 1]	actuation models, e.g. • representation of a pressure force and • a volume force actuation [task b,d of Fig. 1]
feedback flow control element	observer [task f of Fig. 1]	controller [task e of Fig. 1]

(a) (b) (c)
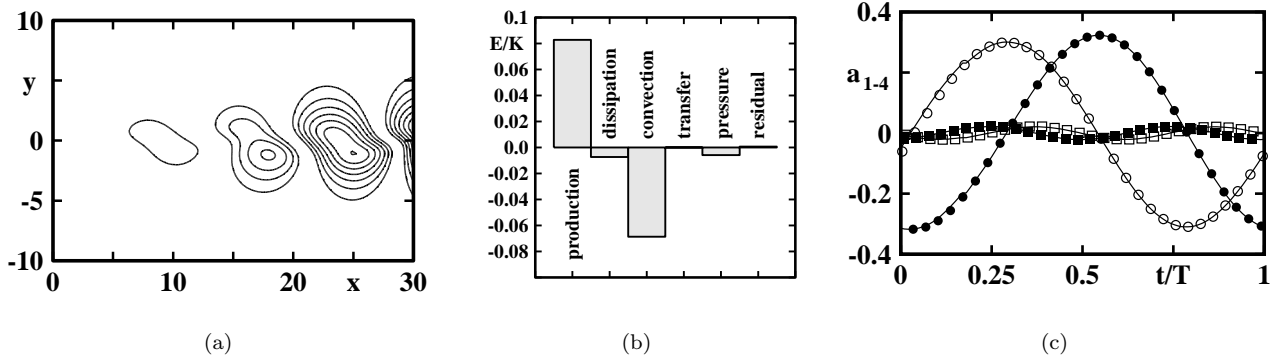
Figure 4. 4-dimensional Galerkin model of laminar 2D Kelvin-Helmholtz vortices.[26] The velocity ratio of both streams is 1:3 and the coordinates are non-dimensionalized with the initial shear-layer thickness. Fig. (a) displays iso-curves of the v component of a DNS snapshot in the computational domain. Fig. (b) visualizes the energy terms in the equation for the turbulent kinetic energy, i.e. production, dissipation, convection term, transfer term, and pressure power. The residual is the sum of these terms and should vanish in a well-resolved DNS. The energy-flow terms are normalized with the fluctuation energy K. Thus, the ordinate represents the fraction of fluctuation energy which is produced or dissipated per convective time unit. Figure (c) illustrates the Fourier coefficients of a 4-dimensional Galerkin model with pressure-term representation. The coefficients a_1 (•), a_2 (∘), a_3 (■) and a_4 (□) depend on the time t which is normalized with the period T. The solid lines are corresponding DNS results.

An energy flow analysis of the fluctuation (see Fig. 4b) reveals that the pressure power is an energy sink which is comparable to viscous dissipation in magnitude. Neglecting the pressure term in the Galerkin model gives rise to a large amplitude over-prediction — even if the number of modes is increased. An analytical pressure-term representation[26, 27] derived from the pressure-Poisson equation is the key enabler for an accurate Galerkin system of the flow (see Fig. 4c).

V.   Turbulent mixing layer

The necessity of a 'subgrid' turbulence representation for high-Reynolds number flow is demonstrated for a LES reference simulation of mixing layer[28] (see Fig. 5). The velocity ratio is the same as for the DNS described in §IV, but the streamwise domain size is almost 5 times larger (measured in shear-layer thicknesses). The inlet tanh profile is 5% perturbed in spanwise direction to enhance the formation of spanwise rib vortices.
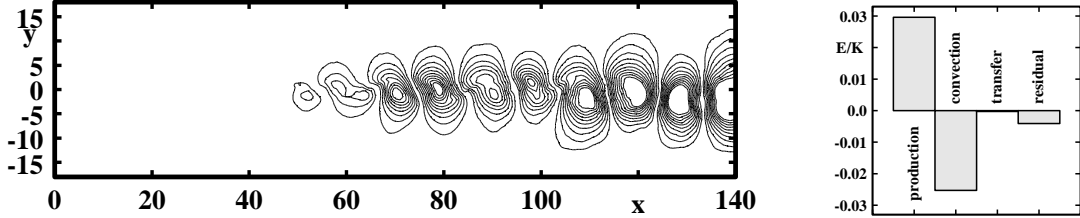

Figure 5. 3D LES simulation of a turbulent mixing layer.[28] **The velocity ratio is 1:3, like in Fig. 4, but the domain is much longer. Fig. (a) represents the iso-curves of the v component of the spanwise averaged flow. Fig. (b) displays energy flow terms. In the LES, a residual energy sink comprising the subgrid dissipation and the pressure power has to be modelled.**

An energy flow analysis (see Fig. 5b) of the LES data reveals an residual energy sink comprising the subgrid dissipation and the pressure power. The sink is modelled in the Galerkin system by the modal eddy viscosity ansatz described in §III. Neglecting this energy sink typically leads to diverging Galerkin solutions — independently of the number of Karhunen-Loève modes.

A 20-dimensional Galerkin model with subgrid turbulence representation resolves already 85% of the fluctuation energy in the LES and captures well the spatio-temporal dynamics of the Kelvin-Helmholtz vortices and resulting vortex merging (see Fig. 6).
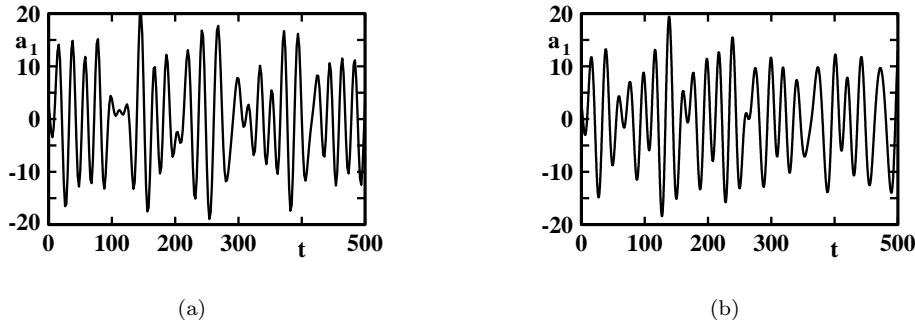

(a)

(b)

Figure 6. 20-dimensional Galerkin model of the LES displayed in Fig. 6. The first Fourier coefficient $a_1(t)$ is illustrated in dependency of the time t for the LES (a) and the Galerkin system (b).

VI.   Transient cylinder wake

The two preceeding sections address additional physics models of the Galerkin method for the attractor dynamics. These generalizations change the coefficients of the Galerkin system (5), but do not require a modification of the Galerkin approximation (3). In this section, the need to enrich the Galerkin phase space is exemplified for the transient cylinder wake behind a circular cylinder.

The standard Galerkin method[8] describes accurately the period vortex shedding at the reference Reynolds number with only 8 Karhunen-Loève modes. Yet, it over-predicts the transient time from the steady solution towards this limit cycle by one order of magnitude.[11] This over-prediction is not too surprising realizing that the Galerkin ansatz is optimized for a single operating condition (I), the periodic vortex shedding. The second operating condition (II) near the steady Navier-Stokes solution is not adequately captured by this

ansatz. This operating condition is well characterized by linear stability theory,[29] i.e. the velocity field can be described by the steady solution, the real part of the most amplified complex eigenmode, and its imaginary part (see Fig. 7a–c). Neither the steady solution nor the stability modes are quantitatively well represented by the Karhunen-Loève decomposition — independently of the number of employed modes[11]!

(a) steady solution

(b) real part of the first stability eigenmode

(c) imaginary part of the first stability eigenmode

(d) averaged natural flow

(e) 1st Karhunen-Loève mode of the natural flow

(f) 2nd Karhunen-Loève mode of the natural flow

(g) averaged actuated flow

(h) 1st Karhunen-Loève mode of an actuated flow

(i) 2nd Karhunen-Loève mode of an actuated flow

(j) shift mode associated with (a) and (d)

(k) actuation mode
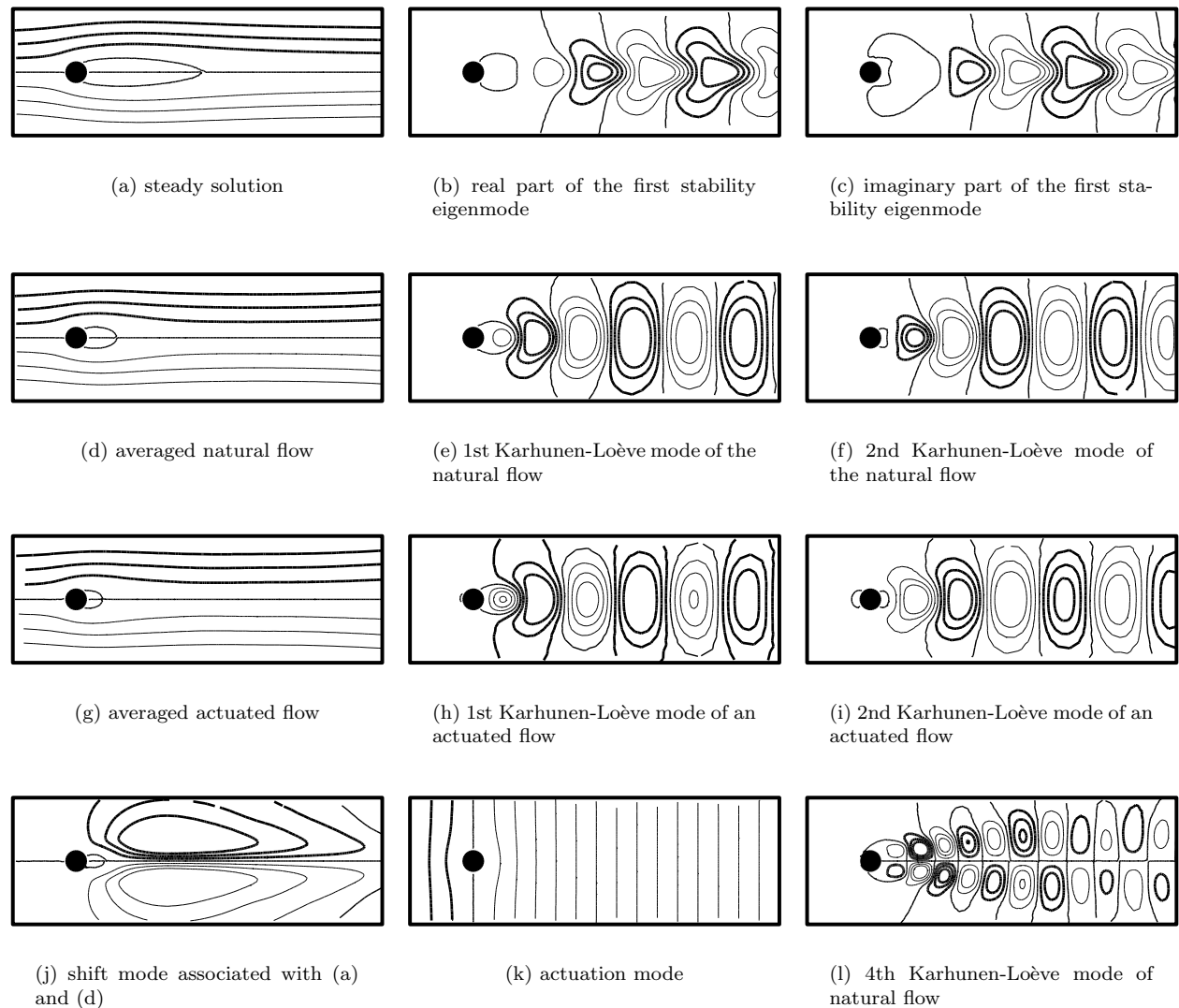
(l) 4th Karhunen-Loève mode of natural flow

Figure 7. Modes for Galerkin models of the natural, transient, and actuated cylinder wake at $Re = 100$. The actuation is provided by a transverse cylinder oscillation at the velocity amplitude 0.1 and the natural shedding frequency (see Ref. 19). In all figures, the flow is visualized with streamlines. Positive values of the streamfunction are highlighted by thick curves.

These three phase-space directions are added to the 8-dimensional Galerkin ansatz (see Fig. 7d–f,l) as orthonormalized non-equilibrium modes. The resulting 11-dimensional model describes well transients from the steady solution to periodic vortex shedding, including the initial growth-rate (see Fig. 8a).

The reason for the large impact of three additional modes can be monitored — again — by an energy flow analysis near the steady solution (see Fig. 8b). The normalized energy flow terms can be determined from the stability eigenmodes in the limit of small amplitudes. The normalized net production ('excess') drives the instability and is twice the growth-rate. Only one third of this net production is resolved within the Galerkin approximation enriched by the shift mode. The standard Galerkin model centered around the mean flow resolves only a tiny fraction of the net production.

The phase-space dynamics of the 11-dimensional Galerkin system are sketched in Fig. 8c. Near the steady solution, the trajectory spirals outward on a plane spanned by the stability eigenmodes. The Reynolds
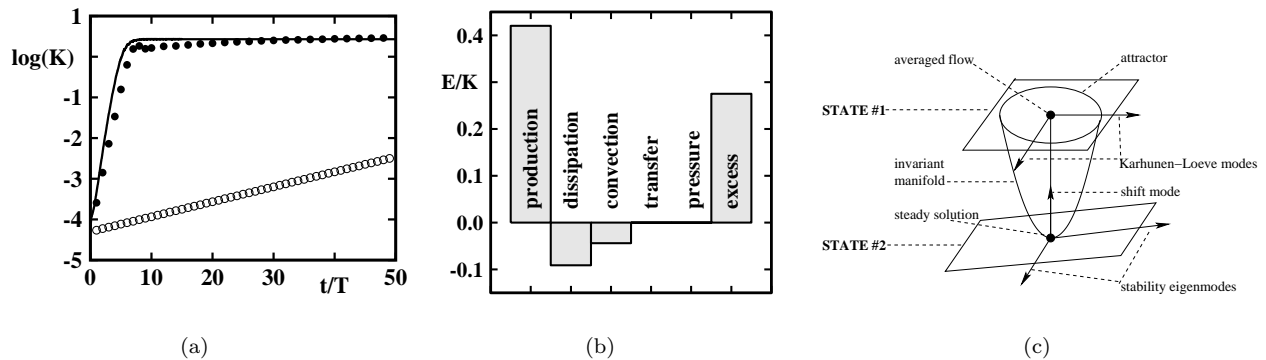
American Institute of Aeronautics and Astronautics Paper 2004-2408

(a)   (b)   (c)

Figure 8. Transient cylinder wake from the neighborhood of the steady solution to the periodic vortex shedding. In Fig. (a), the fluctuation energy is shown as a function of time t normalized with the shedding period T. The curve represents a DNS, the open (solid) symbols the 8-dimensional (11-dimensional) Galerkin model.[11] This model contains modes (b,c,d,e,f,j) and higher harmonic modes like (l) of Fig. 7. In Fig. (b), the normalized energy flow terms are presented for the neighborhood of the steady solution in the mean-field limit. The pressure term can be neglected. The 'excess' drives the instability. In Fig. (c), the role of the modes is sketch for the transient dynamics.

stresses give rise to a non-vanishing shift-mode amplitude (see Fig. 8j) and guide the trajectory on an inertial manifold (paraboloid). During the transient phase, the oscillation 'plane' changes as the limit cycle is approached. These dynamics are a particular case of the more general Fig. 2a. The shift-mode connects two operating conditions whereupon the remaining two non-equilibrium modes allow to calibrate changes of the 'principal axes'. Further details are provided in Ref. 11.

VII.   Actuated cylinder wake

In this section, the implementation of the Galerkin modelling toolbox for the forced cylinder wake is outlined. Two actuations are considered, a volume force behind the circular cylinder and the transverse oscillation of this obstacle.

The uniform volume force is applied in a circular disk of cylinder size on the center line with one diameter distance from the cylinder. A Galerkin model based suppression of vortex shedding is described achieving 83% of the achievable benchmark problem. Further details are provided in Ref. 30.

In addition, suppression of vortex shedding with transverse cylinder oscillations is considered in Part II.[19] The Galerkin model employed in that paper shall briefly be outlined, here. The flow is described in a Cartesian cylinder-fixed coordinate system x, y, where the x-axis is aligned with the flow and the y-axis is perpendicular to the flow and the cylinder axis. In that coordinate system, the cylinder motion y_{cyl} gives rise to a ficticious acceleration force $-\ddot{y}_{cyl}\,\hat{\mathbf{e}}_y$ in the Navier-Stokes equation ($\hat{\mathbf{e}}_y$: unit vector in y direction) and a corresponding term in the Galerkin system (7).

In addition, the cylinder motion leads to a tranverse velocity component $-\dot{y}_{cyl}\,\hat{\mathbf{e}}_y$ in the free-stream condition. This boundary-imposed unsteadiness is incorporated in a single actuation mode $\mathbf{u}'_{inhom} = a_{-1}\mathbf{u}_{-1}$ (see Figs. 2b and 7k). This actuation mode is a rotated basic mode of a mathematical Galerkin method.[21] The first two Karhunen-Loève modes representing the 'flow response' contribution of the fluctuation are visualized in Fig. 7h,i. Here, the cylinder oscillates according to $a_{-1} = -\dot{y}_{cyl} = 0.1\cos\omega t$, where ω represents the natural vortex shedding frequency. Roughly, the 10% fluctuation level in the free-stream leads to a similar increase in the energy level of the Karhunen-Loève modes. The recirculation length of the mean flow (Fig. 7g) is reduced and the activity center of the Karhunen-Loève modes is shifted towards the cylinder.

A 'minimal' four-dimensional Galerkin model is constructed employing a two-dimensional Karhunen-Loève decomposition, the shift mode, and the actuation mode. This minimal model describes well the open-loop forcing of the natural flow and can be used to identify a good controller for the initial suppression.[16] The quantitative accuracy of the model quickly deteriorates with vortex shedding suppression as noted already in Ref. 3. Yet, all qualitative dynamics features remain intact and are found useful for design feedback flow control strategies.[19]

American Institute of Aeronautics and Astronautics Paper 2004-2408

Similar Galerkin model studies have been carried out for the suppression of vortex shedding with oscillatory rotation of the cylinder. Cordier's group[13] has constructed a 40-dimensional Galerkin model for a control design which was validated against simulation. The large dimension of the Karhunen-Loève decomposition has intentionally been achieved using snapshots from an intriguing chirp-forcing transient over a frequency range.

VIII. Conclusions

A Galerkin modelling toolbox is proposed for feedback control design. This toolbox comprises (i) a pressure-term representation for open flows, (ii) a 'subgrid' turbulence representation for LES and high-Reynolds number flows, (iii) non-equilibrium modes for transient dynamics and multiple operating conditions, and (iv) actuation modes for boundary-imposed unsteadiness. These generalizations appear to be sufficient to overcome shortcomings of the standard approach[7] for a large class of simple flow configurations, as indicated by the current investigation and by studies of many other groups.[10,12,13,24,25]

Part II[19] exemplifies a feedback flow control application for the oscillating cylinder wake.

Acknowledgments

References

[1]Roussopoulos, K., "Feedback control of vortex shedding at low Reynolds numbers," *J. Fluid Mech.*, Vol. 248, 1993, pp. 267–296.

[2]Protas, B. and Styczek, A., "Optimal rotary control of the cylinder wake in the laminar regime," *Phys. Fluids*, Vol. 14, 2002, pp. 2073–2087.

[3]Siegel, S., Cohen, K., and McLaughlin, T., "Feedback Control of a Circular Cylinder Wake in Experiment and Simulation," *AIAA-Paper 2003-3571*, 33rd AIAA Fluids Conference and Exhibit,

[4]Gad-el Hak, M., *Flow Control: Passive, Active and Reactive Flow Management*, Cambridge Universty Press, 2000.

[5]King, R., Becker, R., Garwon, M., and Henning, L., "Robust and adaptive closed-loop control of separated shear flows," *AIAA-Paper 2004-2519*, 2nd AIAA Flow Control Conference, Portland, Oregon, U.S.A.

[6]Cordier, L. and Bergmann, M., *Proper Orthogonal Decomposition: An Overview*, VKI Lecture Series 2003-04, Von Kármán Institut for Fluid Dynamics, 2003.

[7]Holmes, P., Lumley, J., and Berkooz, G., *Turbulence, Coherent Structures, Dynamical Systems and Symmetry*, Cambridge University Press, Cambridge, 1998.

[8]Deane, A., Kevrekidis, I., Karniadakis, G., and Orszag, S., "Low-dimensional models for complex geometry flows: Application to grooved channels and circular cylinders," *Phys. Fluids A*, Vol. 3, 1991, pp. 2337–2354.

[9]Ma, X. and Karniadakis, G., "A low-dimensional model for simulating three-dimensional cylinder flow," *J. Fluid Mech.*, Vol. 458, 2002, pp. 181–190.

[10]Jørgensen, B., Sørensen, J., and Brøns, M., "Low-dimensional modeling of a driven cavity flow with two free parameters," *Theoret. Comput. Fluid Dynamics*, Vol. 16, 2003, pp. 299–317.

[11]Noack, B.R., Afanasiev, K., Morzyński, M., Tadmor, G., and Thiele, F., "A hierarchy of low-dimensional models for the transient and post-transient cylinder wake," *J. Fluid Mech.*, Vol. 497, 2003, pp. 335–363.

[12]Galletti, G., Bruneau, C., Zannetti, L., and Iollo, A., "Low-order modelling of laminar flow regimes past a confined square cylinder," *J. Fluid Mech.*, Vol. 503, 2004, pp. 161–170.

[13]Bergmann, M., Cordier, L., and Brancher, J.-P., "Optimal rotary control of the cylinder wake using POD reduced order model," *AIAA-Paper 2004-2323*, 2nd AIAA Flow Control Conference, Portland, Oregon, U.S.A.

[14]Graham, W., Peraire, J., and Tang, K., "Optimal control of vortex shedding usind low-order models. Part I—Open-loop model development," *Int. J. Numer. Meth. Engrng.*, Vol. 44, 1999, pp. 945–972.

[15]Rediniotis, O., Ko, J., and Kurdila, A., "Reduced Order Nonlinear Navier-Stokes Models for Synthetic Jets," *J. Fluids Enrng.*, Vol. 124, 2002, pp. 433–443.

[16]Noack, B.R., Tadmor, G., and Morzyński, M., "Actuation Models and Dissipative Control in Empirical Galerkin Models of Fluid Flows," Paper FrP15.6, *The 2004 American Control Conference*, Boston, MA, U.S.A., June 30–July 2, 2004.

[17]Mokhasi, P. and Rempfer, D., "Optimized sensor placement for urban flow measurement," *Phys. Fluids*, Vol. 16, No. 5, 2004, pp. 1758–1764.

[18]Cohen, K., Siegel, S., Luchtenburg, M., McLaughlin, T., and Seifert, A., "Sensor placement for closed-loop flow control of a 'D' shaped cylinder wake," *AIAA-Paper 2004-2523*, 2nd AIAA Flow Control Conference, Portland, Oregon, U.S.A.

[19]Tadmor, G., Noack, B.R., Morzyński, M., and Siegel, S., "Low-dimensional models for feedback flow control. Part II: Controller design and dynamic estimation," *AIAA-Paper 2004-2409*, 2nd AIAA Flow Control Conference, Portland, Oregon, U.S.A.

[20]Fletcher, C.A.J., *Computational Galerkin Methods*, Springer, New York, 1984.

[21]Noack, B.R. and Eckelmann, H., "A low-dimensional Galerkin method for the three-dimensional flow around a circular cylinder," *Phys. Fluids*, Vol. 6, 1994, pp. 124–143.

[22]Rummler, B., "Zur Lösung der instationären inkompressiblen Navier-Stokesschen Gleichungen in speziellen Gebieten (transl.: On the solution of the incompressible Navier-Stokes equations in some domains)," Habilitation thesis, Fakultät für Mathematik, Otto-von-Guericke-Universität Magdeburg, 2000.

[23]Rempfer, D., "On low-dimensional Galerkin models for fluid flow," *Theoret. Comput. Fluid Dynamics*, Vol. 14, 2000, pp. 75–88.

[24]Rempfer, D., *Kohärente Strukturen und Chaos beim laminar-turbulenten Grenzschichtumschlag (transl.: Coherent structures and chaos of the laminar-turbulent boundary-layer transition)*, Ph.D. thesis, Fakultät Verfahrenstechnik der Universität Stuttgart, 1991, (Part of this work has been published by Rempfer, D. and Fazle, F.H. (1994) in J. Fluid Mech., Vol. 260 & 275).

[25]Couplet, M., Sagaut, P., and Basdevant, C., "Intermodal energy transfers in a proper orthogonal decomposition–Galerkin representation of a turbulent separated flow," *J. Fluid Mech.*, Vol. 491, 2003, pp. 275–284.

[26]Noack, B.R., Papas, P., and Monkewitz, P.A., "Low-dimensional Galerkin model of a laminar shear-layer," Tech. Rep. 2002-01, Laboratoire de Mécanique des Fluides, Département de Genie Mécanique, Ecole Polytechnique Fédérale de Lausanne, Switzerland, 2002.

[27]Noack, B.R., Papas, P., and Monkewitz, P.A., "The need for a pressure-term representation in empirical Galerkin models of incompressible shear-flows," submitted to *J. Fluid Mech.*, 2004.

[28]Comte, P., Silvestrini, J., and Bégou, P., "Streamwise Vortices in Large-Eddy Simulations of Mixing Layer," *Eur. J. Mech. B*, Vol. 17, 1998, pp. 615–637.

[29]Morzyński, M., Afanasiev, K., and Thiele, F., "Solution of the eigenvalue problems resulting from global non-parallel flow stability analysis," *Comput. Meth. Appl. Mech. Enrgrg.*, Vol. 169, 1999, pp. 161–176.

[30]Gerhard, J., Pastoor, M., King, R., Noack, B.R., Dillmann, A., Morzyński, M., and Tadmor, G., "Model-based control of vortex shedding using low-dimensional Galerkin models," *AIAA-Paper 2003-4262*, 33rd AIAA Fluids Conference and Exhibit, Orlando, Florida, U.S.A.